

# Premixed Flames with Nonbranching Chain-Reactions (Structure and Dynamics)

AMABLE LIÑÁN\* and PAUL CLAVIN

## 1. INTRODUCTION

In the recent years, there has been considerable progress in the description of structure and dynamic properties of premixed flames by using asymptotic techniques (for more details see the recent review papers in this field [1-3]). Most of these analyses have been concerned mainly with one step irreversible Arrhenius reactions with an activation energy  $E$  large compared with the thermal energy  $RT_b$  of the mixture at the adiabatic flame temperature  $T_b$ . In this case, the reaction zone is thin and follows a thicker preheated transport zone. Taking advantage of this property, Zeldovich and Frank-Kamenetskii [4] developed in 1938 an approximate solution of the planar flame propagation problem. Bush and Fendell [5] showed much later how the method of matched asymptotic expansions could be used to obtain

corrections to the Zeldovich-Frank-Kamenetskii results that correspond to the dominant order in an asymptotic expansion for large  $E/RT_b$ .

On the basis of the work of Sivashinsky [6], this systematic technique has been extended by Joulin and Clavin [7] to unsteady and nonplanar cases by using the diffusive-thermal model introduced earlier by Barenblatt et al. and Istratov [8]. This model, which neglects the change in the gas density, serves the useful purpose of describing the effects of the heat conductivity and molecular diffusion upon flame dynamics. But, due to the expansion of the gases, the dynamics of flame fronts is also affected by hydrodynamic effects not included in the diffusive thermal model. Such effects were first considered in the pioneering studies of Darrieus [9] and Landau [10], who, neglecting the modification to flame structure by wrinkling the front, considered the flame front as a "locally passive" permeable interface between the burnt and unburnt mixtures, two fluids with constant but different densities. This leads to the

well known hydrodynamic instability of planar fronts. The first pertinent study of the coupling of diffusion and hydrodynamics was carried out in a semiphenomenological analysis by Markstein [11]; but, in the absence of a systematic technique for investigating the structure of wrinkled flames, his study was based on phenomenological considerations that can be questioned. The effect on the flame structure of wrinkles of the front with characteristic size large compared with the flame thickness has been recently investigated by Clavin and Williams [12], by extending previous asymptotic analysis [6, 7] to the case of nonnegligible gas expansion. This analysis has been also extended to the nonlinear case for finite amplitude front corrugations to calculate the change in local burning rate due to front wrinkling and flow inhomogeneities [13, 14]. It turns out that these two effects can be expressed through a unique geometrical scalar, the total flame stretch. Thus, as anticipated by Karlowitz et al. [15], the modification to the normal burning velocity is proportional to the relative change in the element of flame surface; the coefficient of proportionality  $\mathcal{L}$  is proportional to the flame thickness,  $d$ , and is called the Markstein length. The ratio  $\mathcal{L}/d$  depends on the transport properties and chemical kinetics of the reactive mixtures, and its expression is obtained as a result of the analysis. The coupling between diffusive transport mechanisms, heat release, and hydrodynamics has been recently described by Pelcé and Clavin [16], in the linear approximation, to investigate the marginal stability limits of planar fronts propagating downward in the earth's gravity field. In the adiabatic case, the stability limits are completely defined by the Froude number (based upon the acceleration of gravity, the flame thickness  $d$ , and the flame velocity) and two other parameters characterizing the flame, namely, the reduced Markstein number  $\mathcal{L}/d$  and the ratio of the densities of burned and fresh mixtures.

All these results were obtained using, as a first step, a simplified flame model for a one-step overall reaction of reactive mixtures highly diluted with an inert component and with a composition far from stoichiometric. An important effort has been recently devoted to extend these results to

more realistic flame models, including effects of complex diffusive transport processes taking place in multiple components mixtures [17] and the influence of the proximity of flammability limits [18], as well as effects of complex chemistry [2]. As an example, when intermediate species do not verify the quasi-steady state approximation, their transport properties, which are usually different from the main reactive species, may affect the structure and/or dynamic properties of premixed flames. Theoretical analysis of specific examples as the ozone decomposition flame [31] and the hydrogen-oxygen flame [30] have been carried out recently and will appear in future with a comparison with existing numerical results for the structure of steady and planar flames.

It is the purpose of the present analysis to show how flame structure and dynamics are modified when a nonbranching chain reaction is involved in the chemical kinetic mechanisms, as it is the case for most hydrogen-halogen flames. More specifically, we shall be concerned here with reactions that can be modeled by means of the following elementary reactions:

#### *Initiating (dissociation) reaction*



involving the main reactant, a third body, and a radical  $X$  (when necessary, we shall retain the effects of the reverse reaction, with an order  $n$ , that will typically be equal to 2). Reaction (A.1) is responsible for radical production.

#### *Chain (nonbranching) reaction*



which leads to the conversion of the main reactant into products, at a rate determined by the concentration of the radical, whose concentration is not modified by the reaction.

#### *Recombination reaction*



to account for the fact that very often the role of the chain breaking reaction is not played by the reverse of the first reaction, but by a different, sometimes nonelementary reaction. We shall,

however, consider, to simplify the presentation, that (A.1) and (A.3) have the same reaction order,  $n = 2$  for quadratic recombination and  $n = 1$  for the more unusual case of linear recombination.

The initiating reaction is endothermic and has an activation energy larger than that of the chain reaction. The rate of the second reaction is then much larger than that of the initiating reaction, but it is determined by the concentration of radicals. The radical appears in the flame only as a result of the initiating reaction, essentially confined to the hot side of the flame. The recombination reaction, when important at high pressures and low flame temperatures, will lead to an inhibiting of the chain reaction, due to the lowering of radical concentration at the flame.

The ratio of the rates of the initiation and of the chain reactions will be found to be sufficiently small to make the changes in temperature and in main reactant concentration dependent only on the effect of the chain reaction. The incipient thermal effects of the initiation reaction can also be included by proceeding in a way similar to that used in analysing the effect of heat loss on flame structure [7, 19].

The simplified kinetic scheme given above was first introduced by Adams and Stocks [20] (1953) to model the hydrazine decomposition flame. It was used afterwards by Spalding [21] (1955) to model the reactions of hydrogen with halogens, for which the reaction is of the non-chain-branching type.

For example, the  $H_2$ - $Br_2$  reaction can be modeled by the following elementary reaction mechanism:



involving the chain propagating reaction, (B.2) and (B.3), and a chain initiating reaction (B.1); the effects of the reverse reactions are included in the mechanism. Another possible initiating reaction is  $H_2 + M \rightarrow 2H + M$ . However, its activation

energy is sufficiently larger than that of (B.2) that its effect turns out to be negligible.

The reaction constants for the reactions (B.2) and (B.3) are such that, at usual flame temperatures,

$$k_{-3} \ll k_2 \ll k_{-2} \sim k_3,$$

so that

- i. we can neglect the effects of the reverse reaction (B.3) and (B.2),
- ii. we can use the steady state approximation for atomic hydrogen  $H$ , and thus the two reactions (B.2) and (B.3) can be modeled by means of the overall irreversible reaction



with the rate, in moles/unit volume and unit time,

$$\omega' = \{k_2 k_3 n_{Br_2} n_{H_2} / (k_3 n_{Br_2} + k_{-2} n_{HBr})\} n_{Br},$$

if  $n_\alpha$  denotes moles of  $\alpha$  per unit volume.

The overall reaction (B.4) and its associated rate expression must be used together with the initiating reaction (B.1) and its reverse recombination reaction. The resulting kinetic scheme has a structure that, as it occurs for other halogen/ $H_2$  reactions, can be well modeled by the simpler scheme (A.1)–(A.3). Zeldovich [22] (1961) showed how the structure of these halogen flames, modeled by the simplified kinetic scheme, could be described by taking into account that the activation energies of both the initiation and the propagation reaction are large. He neglected the effect of the recombination reaction and gave an approximate analysis of the structure of the flames, which was later refined by Istratov and Librovich [23] (1962).

The purpose of this paper is to provide a general frame work based upon the multiple steps scheme (A.1)–(A.3) helpful for studying every particular flames sustained by a chain nonbranching reaction such as halogen/ $H_2$  flames. Thus we first generalize the analysis of the steady planar flame structure of Zeldovich, Istratov, and Librovich to include the effect of the recombination reaction that can only be neglected at low pressures and high flame

temperatures. In fact we will show that at low flame temperatures we can calculate the radical concentration at the flame, using the quasi-steady approximation, namely, by equating its rate of production and consumption. The steady state approximation for the radicals was introduced by Bodenstein [24] (1913) for the analysis of the kinetics of chemical reactions, and it was widely used by Von Kármán and Penner [26] (1954) and Hirschfelder et al. [25] (1952) in the analysis of the halogen/H<sub>2</sub> flames. The validity of its use in analyzing the H<sub>2</sub>/Br<sub>2</sub> reaction, at high flame temperatures, was soon questioned by Benson [27] (1952). Millán and Da Riva [28] (1962) gave a more detailed analysis of the validity of the steady state approximation in the analysis of flames with nonbranching chain reactions.

We shall see here that indeed the steady state approximation for the radical can be used for flame temperatures below a cross over temperature  $T_b^{**}$  [see Eq. (I.8)] that depends weakly on pressure. In this case the radical concentration is determined as a function of the temperature and concentration of the main reactant; due to the small value of its concentration, relative to that of the reactants, its role in the flame structure and dynamics is limited to its indirect effect in the determination of the rate of the overall reaction.

When the temperature is increased to values close to the cross over temperature  $T_b^{**}$  the radical concentration, although negligible outside the thin reaction zone, can no longer be calculated using the steady state approximation. In what we term the merged regime, for these flame temperatures, the three reactions play a similar role in determining the reaction zone structure and flame speed. The effective activation energy for the flame propagation decreases when the temperature increases above  $T_b^{**}$ .

For temperatures around a second cross over temperature  $T_b^*$  slightly larger than  $T_b^{**}$  the recombination reaction can be neglected in the thin reaction zone, but not in the outer convective diffusive regions. Only for temperatures sufficiently above  $T_b^*$  can the recombination reaction be neglected, and only then will the effective activation energy of the flame propagation cease to decrease, to a value that will change again at high  $T_b$  due to dissociation.

For temperatures close to  $T_b^*$ , or larger, the concentration of the radical in the transport zone is comparable to that of the thin reaction zone, and plays a significant role in the dynamics and stability of the flame.

For high flame temperatures the radical concentration grows so much that the thermal energy used for the dissociation can no longer be neglected. This leads to a lowering of the flame temperature and, hence, of its speed.

We give in Section 2 a description of the steady planar flame structure, beginning in 2.1 with a discussion of the different propagation regimes, based on an order of magnitude analysis presented in Appendix I. The remainder of Section 2 is devoted to the analysis of the slow recombination regime, with a description of the thin reactant consumption and radical production zone in 2.2, and the analysis of the outer transport-recombination zones in 2.2 and 2.3 for the cases of linear and quadratic recombination, respectively. The analysis of the merged regime and of the incipient thermal effects of dissociation are left for Appendix II and Appendix III, respectively.

We give, in Section 3, a description of the wrinkled flame structure and, in Section 4, of the flame front dynamics, for the slow recombination regime, when new effects on the dynamics are to be expected due to the radical diffusivity.

## 2. FLAME SPEED AND STRUCTURE OF STEADY PLANAR FRONTS

### 2.1. The Different Regimes

Let  $T$  be the temperature and  $Y$  and  $X$  the mass fraction of the main reactant and of the radical, respectively. For a steady planar propagation associated with the kinetic scheme A of the introduction, the conservation equations for the species and for the energy take the following form:

$$s_L \frac{dY_L}{dx} - \frac{d}{dx} \left( \rho D_Y \frac{dY_L}{dx} \right) = \rho Z_2 X_L Y_L^r e^{-E_2/RT} - \{ \rho Z_1 Y_L e^{-E_1/RT} - \rho Z_{-1} X_L^n \}, \quad (1a)$$

$$s_L \frac{dX_L}{dx} - \frac{d}{dx} \left( \rho D_x \frac{dX_L}{dx} \right) = \rho Z_1 Y_L e^{-E_1/RT} - \rho (Z_{-1} + Z'_3) X_L^n, \quad (1b)$$

$$s_L \frac{dT_L}{dx} - \frac{d}{dx} \left( \rho D_T \frac{dT_L}{dx} \right) = \frac{Q_2}{C_p} \rho Z_2 X_L Y_L^\nu e^{-E_2/RT} + \left\{ \frac{Q_1}{C_p} \rho (Z_1 Y_L e^{-E_1/RT} - Z_1 X_L^n) + \frac{Q_3}{C_p} \rho Z'_3 X_L^n \right\}, \quad (1c)$$

where  $Z_i$  and  $E_i$  and  $Q_i$  are the prefactor, the activation energy, and the heat release of the  $i$ th reaction, respectively. The  $D$  values are the diffusivities and  $s_L$  is the mass flux, which is constant through the flame and defines the unknown burning rate.  $\rho$  is the density, and  $C_p$  is the specific heat of the reactive mixture; The subscript  $L$  refers to the planar steady state.

We use Fick's law for the diffusion process; this is certainly accurate for a highly diluted mixture. For simplicity, we assume in this analysis, that  $\rho D$ ,  $\rho Z_{-1}$ , and  $\rho Z'_3$  are constant. The temperature dependence of  $\rho D$  can easily be taken into account, even in the dynamical properties [29]. The weak temperature variation of  $\rho Z_{-1}$  and  $\rho Z'_3$  through the flame does not produce significant change in the results. Removing the assumptions,  $\rho Z_{-1}$  and  $\rho Z'_3$  constant, leads to numerical calculations but will not change qualitatively the results. We introduce a reaction order  $\nu \neq 1$  to account partially for the possible nonelementary character of the reaction (A.2). For example, for the hydrogen-bromine reaction when  $\text{Br}_2$  is the limiting component, the production rate associated with the reaction (A.2) has a dependence within the reaction zone of the form  $Y_L/(1 + aY_L)$  where  $a$  is a constant related to the product concentration at the reaction zone. The analysis presented below can be easily adapted to this case, even though it does not have a power law dependence on  $Y_L$ .

The boundary conditions associated to (1) are

$$\begin{aligned} x \rightarrow -\infty (\text{unburnt mixture}): \quad Y_L &= Y_u, \\ X_L &= 0, \quad T = T_u, \\ x \rightarrow +\infty (\text{burnt gases}): \quad Y_L &= 0, \\ X_L &= X_b, \quad T = T_b. \end{aligned} \quad (2)$$

The subscripts  $u$  and  $b$  refer to the unburnt and burnt mixtures, respectively.  $Y_u$  and  $T_u$  are given quantities characterizing the state of the fresh mixture.  $Y_u$  depends in fact on the dilution of the main reactant in the neutral abundant species, as, for example, the nitrogen in air. Notice that because of the effect of the reverse chain reaction (A.2) is neglected, the final equilibrium state leads to  $Y_b = 0$ . Furthermore,  $X_b = 0$  except if the recombination reaction (A.3) and the reverse initiation reaction (A.1) are neglected.

We are going to analyze the realistic case when the initiation reaction (A.1) is slow compared with the unbranched chain reaction (A.2). This is the case when the activation energy  $E_1$  of the initiation reaction is larger than the one,  $E_2$ , of the unbranched chain reaction. Due to the "cold boundary difficulty," the flame propagation problem is meaningful only when  $E_1$  is large enough [3, 32]. When the Zeldovich number  $\beta_1$ , defined by  $\beta_1 = E_1(T_b - T_u)/RT_b^2$ , is assumed to be large compared to unity, an asymptotic analysis for large  $\beta_1$  can be used to calculate the burning rate  $s_L$  that appears as a single eigenvalue of the problem, as for the one overall reaction case [3, 30].

A complete analytical solution can be obtained, for  $n = 1$ , in two limiting cases,  $\beta_2 = 0$  or  $\beta_2 \gg 1$ , where  $\beta_2$  is the Zeldovich number  $\beta_2 = E_2(T_b - T_u)/RT_b^2$ . However, in this paper we shall present the results concerning the general case, where  $n$  is arbitrary and  $\beta_1/\beta_2$  is of order unity with  $\beta_1 > \beta_2 \gg 1$ . In this case the initiation and the unbranched chain reactions are confined to a common thin diffusive-reactive zone of thickness  $d/\beta_2$ , separating two much thicker zones, of thickness  $d = \rho D_T/s_L$ , where convection, diffusion, and radical recombination are balanced (see Fig. 1). We shall present the results concerning  $n = 1$  and  $n = 2$ .

One can anticipate that, due to the assumption  $E_1 > E_2$ , and for realistic values of the frequency

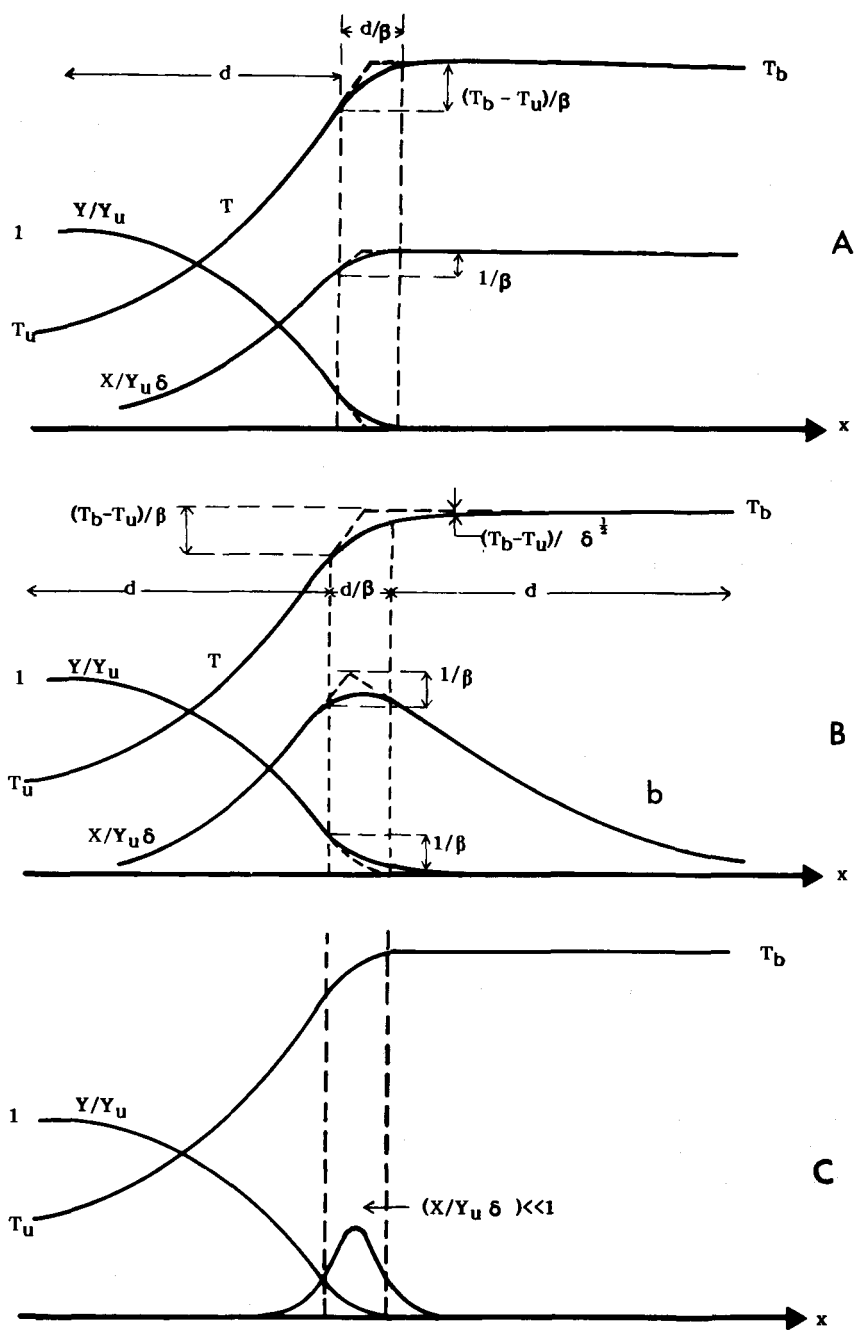


Fig. 1. Temperature and species profiles across laminar flame: (A) negligible recombination; (B) slow recombination; (C) quasi-steady state approximation.

factors  $Z_1$ ,  $Z_2$ , and  $Z_3'$ , we can neglect, in the conservation equations for the main reactant and the temperature, the terms in curly brackets associated with the initiation and recombination reactions, retaining in these equations only the effect of the chain reaction. In that case, the temperature downstream of the thin reactive zone is approximatively constant and equal to the burnt gas temperature given by

$$T_b = T_u + Y_u Q_2 / C_p \quad (3)$$

that we shall call the flame temperature, because the temperature of the reaction zone is equal to  $T_b$ , at first order for large values of  $\beta_2$  (see Fig. 1).

To define more precisely the limit of validity of these approximations, let us introduce the reaction frequencies  $\Omega_1$  and  $\Omega_2$  of the initiation and of the unbranched-chain reactions, evaluated at the flame temperature  $T_b$ :

$$\Omega_1 = Z_{1b} \exp(-E_1/RT_b),$$

$$\Omega_2 \equiv \Omega_1/\delta = Y_u^\nu Z_{2b} \exp(-E_2/RT_b). \quad (4)$$

As in the early works of Zeldovich [22] and of Istratov and Librovich [23], who neglected the recombination and the reverse initiation reaction ( $Z_{-1} = Z_3' = 0$ ), we consider the realistic case where the initiation reaction is so slow compared to the unbranching chain reaction that  $\delta$  is negligibly small compared to one,  $\delta \ll 1$ . In the limit of large activation energies this is consistent with the assumption  $\beta_1 > \beta_2$ , because in this case

$$\delta = \sigma(\beta_2^{-m}), \quad \forall m \in \mathbb{Z}^+. \quad (5)$$

Then, as it is shown in Appendix I, the reduced radical mass fraction,  $c = X/Y_u$ , and the ratio of the rates of the initiation and of the unbranching chain reactions are of order  $\delta^{1/2}$ :

$$c_L = X_L/Y_u = O(\delta^{1/2} \beta_2^{(\nu-1)/2}),$$

$$Z_{1b} Y_L e^{-E_1/RT_b} / Z_{2b} X_L Y_L^\nu e^{-E_2/RT_b}$$

$$= O(\delta^{1/2} \beta_2^{(\nu-1)/2}). \quad (6)$$

Furthermore our main analysis will be limited to the cases where  $Z_{-1} + Z_3$  is small enough so that  $\rho(Z_{-1} + Z_3)X_L^n \leq \rho Z_1 Y_L e^{-E_1/RT}$  (see Appendix

I), and thus only the production term associated with  $Z_2$  is to be considered in the equations of conservation for the main reactant and for the energy. Thus, in the following, we shall omit the curly bracket terms in Eqs. (1). The effects of these terms on the flame structure become important at flame temperatures high enough to make  $\delta = O(1/\beta_2^{1+\nu})$  corresponding to  $c_L = O(1/\beta_2)$ : the corresponding flame structure is briefly described in Appendix III. In the case characterized by the relation (6) where the curly bracket terms are negligible in Eqs. (1), it is clear from (1b) that the reverse initiation reaction and the recombination reaction play similar role and appear only through the sum  $Z_{-1} + Z_3'$ . To simplify the notation we shall denote this sum as  $Z_3$  and call it in the following simply by the "recombination,"  $Z_3 = Z_{-1} + Z_3'$ .

In this paper we first generalize the analyses [22, 23] of the steady planar flame structure to include the effect of a linear or quadratic recombination reaction for values of the frequency factor  $\Omega_3 = Z_3 Y_u^{n-1}$  ranging from zero ( $\Omega_3 = 0$ ) to values large enough ( $\Omega_3 \gg \Omega^{**}$ ) that the steady state approximation can be used for the radical species (see Appendix I). In this last case, the radical concentration  $X_L$  is simply obtained by equating the chemical production term  $\rho_b Z_1 Y_L e^{-E_1/RT_b}$  to the chemical consumption by recombination,  $\rho_b Z_3 X_L^n$ ,

$$X_L/Y_u = (\Omega_1/\Omega_3)^{1/n} (Y_L/Y_u)^{1/n}, \quad (7)$$

and the flame propagation problem reduces to the simplest case involving only one overall irreversible exothermal reaction order of  $\nu + (1/n)$  in the main reactant, with a prefactor  $Z = Z_2(Z_1/Z_3)^{1/n}$  and an activation energy  $E = E_2 + E_1/n$ . Using the classical asymptotic theory [4] one obtains for the burning rate

$$s^2 = 2\Gamma_{\nu+1/n} \beta^{-\nu-1-1/n} \rho D_T \rho_b \Omega_2 (\Omega_1/\Omega_3)^{1/n}$$

$$= 2\Gamma_{\nu+1/n} \beta^{-\nu-1-1/n} \rho_b Y_u^\nu Z_2$$

$$\times \left( \frac{Z_1}{Z_3 Y_u^{n-1}} \right)^{1/n} e^{-E/RT_b}, \quad (8)$$

where  $\beta = [E/(RT_b^2)](T_b - T_u)$  and  $L_Y = D_T/D_Y$  are the reduced activation energy and the

Lewis number of the main reactant, respectively.  $\Gamma_x$  is the gamma function of  $x$ , which is equal to  $(x!)$  for  $x \in \mathbb{Z}^+$ . Relation (8) holds only when the recombination reaction is very fast and in this case, the diffusive properties of the radical do not play any role. It can be anticipated that this cannot be the case in the opposite case, when the recombination reaction is slow enough to be ignored in the reaction zone but not outside. On the basis of the order of magnitude analysis of Appendix I, we define a critical value  $\Omega_3^*$  of the frequency factor of the recombination reaction, by

$$\Omega_3^* = \beta_2^{-2+(1-\nu)n/2} \Omega_1^{1-n/2} \Omega_2^{n/2}. \quad (9)$$

When  $\Omega_3/\Omega_3^* = O(1)$  the recombination reaction can play a role only outside the thin reactive zone. In this case the characteristic time  $\Omega_3^{-1}$  of the recombination reaction has the same order of magnitude as the transit time  $\rho_u d/s_L$  and the diffusive properties of the radical are expected to affect the final results. In this notable limiting case when  $\Omega_3/\Omega_3^* = O(1)$  the flame structure is sketched in Fig. 1b. Contrary to the case when the recombination reaction is neglected,  $\Omega_3 = O$  (see Fig. 1a), there is a downstream nontrivial outer zone where the radical decreases to zero. The recombination leads there to small relative changes of  $T$  and  $Y$  of order  $\sqrt{\delta}$ , which are neglected in this analysis when  $\delta$  is assumed exponentially small. The relative changes in the radical concentration in the thin reactive zone are, as it is the case for  $Y$  and  $T$ , of order  $1/\beta_2$ .

With increasing values of  $\Omega_3$  above  $\Omega_3^*$  the radical concentration decreases, and for values of  $\Omega_3$  of the order of  $\Omega_3^{**}$ , defined in Appendix I, a merged regime appears, for which the radical recombination term in Eq. (1b) becomes, inside the thin reactive zone, of the same order of magnitude as the radical production term, and the radical recombination is negligible outside. In this merged regime,  $\Omega_3/\Omega_3^{**} = O(1)$ , the relative changes of the radical concentration in the thin reactive zone are of order one (see Fig. 1c). For the intermediate values of  $\Omega_3$ ,  $\Omega_3^* \ll \Omega_3 \ll \Omega_3^{**}$ , the merged regime ( $\Omega_3 \sim \Omega_3^{**}$ ) and the slow recombination regime ( $\Omega_3 \sim \Omega_3^*$ ) match. Furthermore, the merged regime leads to the steady state approximation for the radical when  $\Omega_3/\Omega_3^{**} \gg 1$ .

Notice that both  $\Omega_3^*$  and  $\Omega_3^{**}$ , defined by (1.5) and (1.8), are strongly increasing functions of the flame temperature if  $n \leq 2$ , which are the physically relevant cases. As the temperature dependence of  $\Omega_3$  is usually small, the relations  $\Omega_3 = \Omega_3^*$  and  $\Omega_3 = \Omega_3^{**}$  define the cross over flame temperatures  $T_b^*$  and  $T_b^{**}$ , slightly smaller than  $T_b^*$ . When  $T_b < T_b^{**}$  the fast recombination regime described by the steady state assumption holds. When  $T_b$  is close to  $T_b^{**}$  we have the merged regime. When  $T_b$  is close to or larger than  $T_b^*$  we have the slow recombination regime that is the main subject of this paper. Because the ratios  $\Omega_3/\Omega_3^*$  and  $\Omega_3/\Omega_3^{**}$  are usually linearly dependent on the pressure, the cross over temperatures  $T_b^*$  and  $T_b^{**}$  are expected to increase slightly with increasing pressure.

As the fast recombination case is well known, and simply described by (8), it is sufficient for the study of the effect of the recombination to investigate in detail the slow recombination regime,  $\Omega_3/\Omega_3^* = O(1)$ , the merged regime ensuring simply the continuous path to the steady state approximation. Thus, we shall only present here the detailed analysis of the slow recombination regime, which is described by the notable limiting case  $\beta_1 > \beta_2 \rightarrow \infty$ ,  $\Omega_3/\Omega_3^* = O(1)$  with  $\delta = \Omega_1/\Omega_2$  transcendently small.

## 2.2. The Reactive Zone Structure

We choose the origin of the  $x$  axis inside the inner zone, the structure of which is controlled by the following set of equations:

$$\begin{aligned} \rho D_T \frac{d^2 \theta}{dx^2} &= -\rho D_Y \frac{d^2 y}{dx^2} \\ &= -\rho_b \Omega_2 c_f y^\nu e^{\beta_2(\theta-1)}, \end{aligned} \quad (10a)$$

$$-\rho D_X \frac{d^2 c}{dx^2} = \rho_b \Omega_1 y e^{\beta_1(\theta-1)}, \quad (10b)$$

where

$$\begin{aligned} y &= Y/Y_u, \quad c = X/Y_u, \\ \theta &= (T - T_u)/(T_b - T_u). \end{aligned} \quad (10c)$$

The subscript f denotes conditions immediately



downstream of the thin reactive zone. The convective terms can be neglected in this zone and the Arrhenius exponent can be linearized around  $T = T_b$ .

By a direct integration of (10a) through the inner zone, the jump in total enthalpy flux is found to be zero. Namely,

$$\left[ \rho D_T \frac{d\theta}{dx} + \rho D_Y \frac{dy}{dx} \right]_+ = 0. \quad (11a)$$

Anticipating that the reaction has gone to completion,  $y = 0$  in the burnt gases, and that there is no temperature gradient,  $d\theta/dx = 0$ , downstream of the reaction zone, then one obtains the outcoming heat flux immediately upstream of the reaction zone:

$$-\rho D_T \frac{d\theta}{dx} \Big|_- = (2\Gamma_\nu L_Y^\nu \rho D_T)^{1/2} \beta_2^{-(\nu+1)/2} \times \rho_b^{1/2} (\Omega_2 c_f)^{1/2}. \quad (11b)$$

The condition  $\theta = 1$  has been used downstream to obtain (11b). However, the relations (11a) and (11b) are still valid when, due to wrinkling or unsteady effects, the temperature just downstream of the thin reaction zone changes from  $T_b$  to a value  $T_f$  that should be used in evaluating  $\Omega_1$  and  $\Omega_2$ . The same is true when calculating the jump in the radical flux through the thin reactive zone, which is given by Eq. (11d), obtained by a direct integration of (10b) together with the following first order equation, (11c), for  $y$  inside the reaction zone,

$$\frac{dy}{dx} = -(2\rho_b/\rho D_T)^{1/2} L_Y^{1+\nu/2} \beta_2^{-(\nu+1)/2} (\Omega_2 c_f)^{1/2} \times \{1 - (\psi + 1)e^{-\psi}\}^{1/2}, \quad (11c)$$

with  $\psi = y\beta_2/L_Y$ . Equation (11c) is obtained in a way similar to (11b).

$$-\rho D_X \left[ \frac{dc}{dx} \right]_+ = M = \Omega_1 (c_f \Omega_2)^{-1/2} C, \quad (11d)$$

with  $C$  defined by

$$C^2 = b^2 \rho_b \beta_2^{\nu-3} \rho D_T / 2 L_Y^{\nu-2}$$

and  $b$ , a function only of  $\nu$  and  $E_1/E_2$ , defined by

$$b = \int_0^\infty \left\{ 1 - \sum_{i=0}^\nu \frac{\nu!}{i!} \psi^{\nu-i} e^{-\psi} \right\}^{-1/2}$$

$$\times e^{-\psi E_1/E_2} d\psi, \quad \nu \in Z^+,$$

that is equal to 2 for  $\nu = 1$  and  $E_1 = E_2$ , and behaves as  $\sqrt{2}E_2/E_1$  for large values of  $E_1/E_2$ . Notice that, in the steady planar case, one has  $\theta = 1$  for  $x \rightarrow +\infty$ , so that  $y = L_Y(1 - \theta)$  everywhere in the reaction zone.

### 2.3. The Linear Recombination Case, $n = 1$

The outer flame structure is given by the solution of (1) with the production terms with large activation energies neglected upstream, because the reaction are thermally quenched, and downstream, because there is no more reactant,  $Y = 0$ . Thus, the only production term left is the radical recombination which must be retained in Eq. (1b). At the dominant order, for large  $\beta_2$ , the solution for  $Y$  and  $T$  are given by

$$y_L = Y_L/Y_u = 1 - e^{L_Y(x/d)},$$

$$\theta_L = \frac{T_L - T_u}{T_b - T_u} = e^{x/d} \quad \text{for } x < 0, \quad (12)$$

$$y_L = 0, \quad \theta_L = 1 \quad \text{for } x > 0.$$

The solution for the radical concentration depends on the order of the radical recombination  $n$ . Let us first present the result for  $n = 1$ :

$$n = 1 \begin{cases} c_L = c_{fL} e^{\nu_L x/(d)} & \text{for } x > 0 \\ c_L = c_{fL} e^{\nu_L L - (x/d)} & \text{for } x < 0 \end{cases} \quad (13)$$

with

$$\nu_{L\pm} = (1 \mp \sqrt{1 + \Delta}) L_X / 2,$$

where  $D_T/D_X = L_X$  is the Lewis number based on the molecular diffusivity of the radical, and where the Damköhler number  $\Delta$ , appearing in  $\nu_{L\pm}$ ,

$$\Delta = 4\rho_b \Omega_3 \rho D_X / s_L^2, \quad (14)$$

is roughly the ratio of the transit time across the

flame and the characteristic reaction time for the recombination. The concentration  $c_{fL} Y_u$  of the radical at the thin reactive zone and the burning rate  $s_L$  can be calculated only by using the results (11) of the study of the thin reactive zone structure. From (12) we obtain

$$\left. \frac{d\theta}{dx} \right|_- = -s_L/\rho D_T, \quad (15)$$

which provides, by using (11b), a first relation between  $s_L$  and  $c_{fL}$ :

$$s_L/(\Omega_2 c_{fL})^{1/2} = B \equiv \{2\rho_b \Gamma_\nu L_Y^\nu \rho D_T \beta_2^{-(\nu+1)}\}^{1/2}. \quad (16)$$

A second relation to calculate  $s_L$  and  $c_{fL}$  can be obtained from (11d) by using the results of (13),

$$\rho D_X \left[ \frac{dc_L}{dx} \right]_-^+ = -c_{fL} (1 + \Delta)^{1/2}, \quad (17)$$

so that we obtain

$$c_{fL}^{3/2} s_L \Delta = C \Omega_1 \Omega_2^{-1/2}, \quad (18)$$

where the scalar  $C$  was defined before by

$$C^2 = b^2 \rho_b \rho D_T / 2 L_Y^{\nu-2} \beta_2^{3-\nu}. \quad (18')$$

When the recombination reaction is neglected,  $\Omega_3 = 0$ , (16) and (18) yield the following values for the burning rate  $s_{L0}$  and for the reduced radical concentration  $c_{fL0}$  at the reactive zone,

$$s_{L0} = (2\rho_b^2 \Gamma_\nu^{3/2} \rho^2 D_T^2 L_Y^{\nu+1} b)^{1/4} \times \beta_2^{(3+\nu)/4} (\Omega_1 \Omega_2)^{1/4}, \quad (19a)$$

$$c_{fL0} = \{b L_Y^{1-\nu} / 2 \Gamma_\nu^{1/2}\}^{1/2} \beta_2^{(\nu-1)/2} (\Omega_1 / \Omega_2)^{1/2}, \quad (19b)$$

or equivalently

$$s_{L0}^4 = B^3 C \Omega_1 \Omega_2, \quad c_{fL0}^2 = C B^{-1} \Omega_1 / \Omega_2, \quad (19')$$

which have been previously obtained for  $\nu = 1$  by Istratov and Librovich [23]. Notice that the flame speed (19a) would result for a one step overall reaction for the main reactant, with an activation energy  $(E_1 + E_2)/2$ . It is also worthwhile noting that in these results, concerning the planar steady

state propagation, the diffusive properties of the radical do not enter. Because of the presence of radicals in the outer zones (see Figs. 1a and 1b), it can be easily anticipated that the dynamical properties of such flames cannot be modeled by such an overall reaction, and they will depend on the diffusion coefficient  $D_X$  of the radical, unless the recombination reaction is so fast that we are in the merged regime, or the steady state assumption for the radical concentration holds.

For a nonzero value of the Damköhler number  $\Delta_0$ ,

$$\Delta_0 = 4\rho_b \Omega_3 \rho D_X / s_{L0}^2, \quad (20)$$

the burning rate  $s_L$  and the radical concentration  $c_{fL}$  are no longer given by (19) but by

$$c_{fL}/c_{fL0} = (s_L/s_{L0})^2, \quad (21a)$$

$$(s_L/s_{L0}) \{1 + \Delta_0 (s_L/s_{L0})^{-2}\} = 1. \quad (21b)$$

Notice that the Damköhler number  $\Delta$  that appears in  $\nu_{L\pm}$  (13) is related to  $\Delta_0$  by

$$\Delta = \Delta_0 (s_L/s_{L0})^{-2} \quad (22)$$

and thus,  $(s_L/s_{L0})$  and  $\Delta$  are functions of  $\Delta_0$  (shown in Fig. 2). Notice that when (19a) is used,  $\Delta_0$  defined by (20) is seen to be directly related to  $\Omega_3/\Omega_3^*$ , with  $\Omega_3^*$  given by (9). For  $n = 1$  one obtains

$$\Delta_0 = 4 \{2b \Gamma_\nu^{3/2} L_Y^{(5-\nu)/2} L_X^2\}^{-1/2} \Omega_3 / \Omega_3^*. \quad (23)$$

Notice also the linear dependence of  $\Delta_0$  on  $L_X^{-1}$  that did not appear in  $s_L$  and  $c_{fL}$  when  $\Omega_3$  is zero [see Eq. (19)]. It is clear, from the results plotted in Fig. 2, that the effect of the radical recombination is to decrease the flame speed and the concentration of radicals, now depending on the diffusive properties of the radical. In fact  $s_L$  and  $c_{fL}$  decrease when increasing  $\Omega_3$  or the molecular diffusion coefficient  $D_X$  of the radical. Notice also that, according to (21),  $(s_L/s_{L0})^2 \rightarrow 1$  for  $\Delta_0 \rightarrow 0$  and  $(s_L/s_{L0})^2 \rightarrow \Delta_0^{-1/2}$  for  $\Delta_0 \rightarrow \infty$ . Thus the effective overall activation energy is now changing, through  $\Delta_0$ , when  $\Omega_3/\Omega_3^*$  increases from 0 to values large compared with one. When according to (1.5) and (1.8),  $\Omega_3/\Omega_3^*$  becomes of the order  $\beta_2^{3/2}$  we reach the merged regime, and the

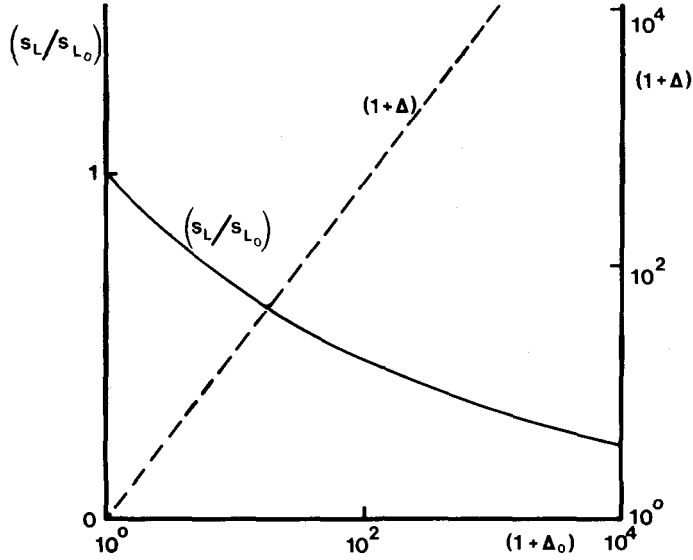


Fig. 2. Reduced flame speed  $(s_L/s_{L0})$  versus Damköhler number  $\Delta_0$  [see Eq. (20)] for  $n = 1$ .

relations (21) are no longer valid. The overall activation energy begins to increase up to the value  $E_1 + E_2$  associated with the steady state approximation that leads to (8).

It is worthwhile to point out how the radical profiles (13) depend on  $\Omega_3/\Omega_3^*$  (through  $\Delta$ ). For small values of  $\Omega_3/\Omega_3^* \ll 1$ , the effects of the radical recombination reaction can be neglected in the upstream preheated zone but are felt in a long convective-recombination region, of thickness  $d/L_X\Delta_0$ , which follows the thin radical production zone and where the diffusive terms can be neglected. For large values of  $\Omega_3/\Omega_3^*$  the radical concentration profiles shrink toward a thin region of thickness  $d/L_X\Delta_0^{2/3}$ . The merged regime defined by  $\Omega_3/\Omega_3^* = O(\beta_2^{3/2})$  is in fact associated to a thickness of the radical recombination of the order of the thickness of the thin reactive zone  $d/\beta_2$ .

#### 2.4. Quadratic Recombination Case, $n = 2$

In that case (17) and (18) are no more valid. The outer equation for the radical profile is, according to (1b),

$$s_L \frac{dc_L}{dx} - \rho D_X \frac{d^2 c_L}{dx^2} + \rho_b \Omega_3 c_L^2 = M \delta(x), \quad (24)$$

where the strength  $M$  of the delta function is given by Eq. (11d), in order to satisfy the jump condition across the inner reaction zone. Equation (24) has to be solved with the boundary conditions  $c_L(x = \pm \infty) = 0$ .

A similar problem has already been treated by Liñán [33], who solved numerically the following problem,

$$\begin{aligned} \phi_\xi - \phi_{\xi\xi} + m\phi^2 &= \delta(\xi); \\ \phi &= 0 \quad \text{for } \xi \rightarrow \pm \infty \end{aligned} \quad (25)$$

to obtain a relation between the value of  $\phi$  at  $\xi = 0$ ,  $\phi_f$ , and  $m$ . The relating function  $\phi_f(m)$  can be well correlated by the closed form expression

$$m\phi_f = 3(1 - \phi_f^2)/8\phi_f^2(1 + \phi_f^2/2) \quad (26)$$

having the correct asymptotic form

$$\phi_f \approx 1 - 3m/2 \quad \text{for } m \rightarrow 0,$$

$$\phi_f \approx (3/8m)^{1/3} \quad \text{for } m \rightarrow \infty.$$

Equations (24) and (11d) correspond to Eq. (25) for

$$\begin{aligned} \xi &= xs_L/\rho D_X, & \phi &= c_L s_L/M, \\ \phi_f &= c_{fL} s_L/M, & m &= \rho D_X \rho_b \Omega_3 M/s_L^3. \end{aligned} \quad (27)$$

According to the definition of  $M$  and  $C$  [see (11d) and (18')], one can write

$$M = C\Omega_1(c_{fL}\Omega_2)^{-1/2}. \quad (28)$$

The relations (26) and (27) provide the new relation between  $\phi_f$  and  $s_L$  that replaces (18). This new relation has to be used with (16), which is still valid for  $n = 2$ , and which can be written as

$$c_{fL} = B^{-2}\Omega_2^{-1}s_L^2, \quad (29)$$

with  $B$  given by Eq. (16). From (28) and (29) we obtain

$$M = CB\Omega_1/s_L. \quad (30)$$

Equations (29) and (30) together with (27) give

$$\begin{aligned} \phi_f &= s_L^4/B^3 C\Omega_1\Omega_2 = (s_L/s_{L0})^4 \\ &= (c_{fL}/c_{fL0})^2, \end{aligned} \quad (31a)$$

$$\begin{aligned} m &= \rho D_X \rho_b \Omega_3 C B \Omega_1 s_L^{-4}, \\ m\phi_f &= \Delta'_0 = (\Omega_3/\Omega_3^*)(2\Gamma_\nu L_X L_Y^\nu)^{-1}, \end{aligned} \quad (31b)$$

where  $\Omega_3^*$  is given by (9), with  $n = 2$ ,

$$\Omega_3^* = \Omega_2 \beta_2^{-(1+\nu)}. \quad (32)$$

Thus when (31a) and (31b) are introduced into (26) one obtains a relation similar to (21) involving a nondimensional recombination parameter  $\Delta'_0 = m\phi_f$  given by (31b). The corresponding curve  $s_L/s_{L0}$  versus  $\Omega_3/\Omega_3^* \sim \Delta'_0$  has a qualitative behavior similar to that for the case  $n = 1$ ; the effective overall activation energy is changing with the flame temperature, through  $\Omega_3/\Omega_3^*$ , growing from  $[(E_1/2) + (E_2/2)]$  to  $[(E_1/2) + (3/4)E_2]$  when  $(\Omega_3/\Omega_3^*)$  increases from 0 to values large compared to one. However, when  $\Omega_3/\Omega_3^*$  becomes of the order  $\beta_2^2$  we encounter the merged regime; then the effective activation energy begins to increase up to the value  $(E_1/2) + E_2$ , corresponding to the steady state approximation resulting in (8).

### 3. STRUCTURE OF WRINKLED FLAMES

We present here an analysis of the structure of wrinkled flames. The reader may skip the technical part of this section in a first reading, and

proceed to the following section where the results are presented in a self-consistent way.

When the flame front is wrinkled the flame structure is modified by transverse fluxes of energy and mass, which appear inside the preheated zone in a tangential direction to the surface of the front. Due to the expansion of the gas through the flame, convective transverse fluxes are also generated, in addition to the diffusive ones, as a result of the deflection of the streamlines across the flame. Unsteady or strain effects of the flow field lead to changes in the flame structure.

The wrinkling of the front induces inviscid changes in the flow field outside the flame in regions with the length scale of the wrinkles. When this length is large compared to the flame thickness  $d$ , the flame structure can be described analytically in terms of the characteristics of the flow field immediately upstream of the flame [12, 13]. Then, jump conditions concerning the flow are obtained by the analysis of the flame structure; these can afterward be used to determine the induced velocity field and thus the motion of the flame front. This interaction between the flame structure and the outer inviscid hydrodynamics has already been described for an Arrhenius one step irreversible reaction [16]. Because no significant changes in the structure of the outer flow field are introduced by the kinetics, only the wrinkled flame structure is addressed here. As in the previous studies, the Lewis number  $L_Y$  of the main reactant controls the modification of the temperature of combustion and is chosen to be close to the unity,  $L_Y - 1 = O(\beta_2^{-1})$ ,

$$L_Y = 1 + \frac{l}{\beta_2}, \quad (33)$$

to ensure that the relative modification of the temperature of combustion is of order  $\beta_2^{-1}$ ; the local burning rate is only modified by a factor of order unity for large values of  $\beta_2$  ( $\beta_2 \rightarrow \infty$ ). This is not a strong limitation for the main reactant of the usual reactive mixtures. However, some radicals as H are very light and their Lewis number can differ significantly from unity, so that in our analysis  $L_X - 1$  is not necessarily considered as a small quantity,  $L_X - 1 = O(1)$ .

When the nondimensional coordinates<sup>1</sup> ( $\xi, \eta, \tau$ ) defined by  $\xi = (x - \alpha)/d$ ,  $\eta = z/d$ ,  $\tau = tu_L/d$ , are introduced in the moving frame,  $x = \alpha(z, t)$  being the equation for the flame front surface defined by the location of the inner zone  $Y = 0$ , the linearized version of the energy and species conservation equations take, outside the reaction zone, the following form (for linear recombination):

$$r_L y_\tau + y_\xi + (s + L_Y^{-1} \alpha_{\eta\eta}) y_{L\xi} = L_Y^{-1} (y_{\xi\xi} + y_{\eta\eta}), \quad (34a)$$

$$r_L \theta_\tau + \theta_\xi + (s + \alpha_{\eta\eta}) \theta_{L\xi} = \theta_{\xi\xi} + \theta_{\eta\eta}, \quad (34b)$$

$$r_L \phi_\tau + \phi_\xi + (s + L_X^{-1} \alpha_{\eta\eta}) \phi_{L\xi} = L_X^{-1} (\phi_{\xi\xi} + \phi_{\eta\eta}) - \phi L_X \Delta/4, \quad (34c)$$

where here  $y$ ,  $\theta$ , and  $\phi$  are the perturbations of the reduced mass fraction of the main reactant, the reduced temperature, and the reduced mass fraction of the radical, respectively:

$$Y/Y_u = y_L + y, \quad (T - T_u)/(T_b - T_u) = \theta_L + \theta, \\ c/c_{fL} = \phi_L + \phi.$$

Here the unperturbed profiles (12) and (13) have the form

$$y_L = 1 - e^{\xi L_Y}, \quad \theta_L = e^\xi, \\ \phi_L = e^{\xi \nu_L -}: \quad \xi < 0, \quad (35a)$$

$$y_L = 0, \quad \theta_L = 0, \\ \phi_L = e^{\xi \nu_L +}: \quad \xi > 0. \quad (35b)$$

$r_L$  gives the unperturbed density distribution.  $s$  is the perturbation of the  $\xi$  component of the nondimensional mass flux in the moving coordinate system, written with the steady planar burning rate  $s_L$  as unit.  $s$  satisfies the linearized continuity equation, which can be written in the moving frame as

$$r_\tau + s_\xi + (r_L v)_\eta = 0, \quad (36)$$

where  $r$  is the perturbation of the reduced density

$\rho/\rho_u$ , which, according to the usual negligibly small Mach number assumption of the flame theory, is related to  $\theta$  by the perfect gas law;

$$r = -\theta r_L^2 \gamma / (1 - \gamma), \quad (37)$$

where  $\gamma = (T_b - T_u)/T_b$  is the gas expansion parameter and  $r_L = \{1 + e^\xi \gamma / (1 - \gamma)\}^{-1}$  for  $\xi < 0$  and  $r_L = (1 - \gamma)$  for  $\xi > 0$ . Let  $U$  and  $v$  appearing in (36) be the perturbations of the reduced  $x$  and  $z$  components of the flow velocity in the laboratory frame, written with the flame velocity  $u_L$  as unit:

$$s = r_L (U - \alpha_\tau) + r u_L. \quad (38)$$

As in the previous analysis [12, 13, 16] the attention is restricted to situations where the wavelengths  $\Lambda$  of the wrinkles of the front are large compared to the flame thickness  $\epsilon = d/\Lambda \ll 1$ . Then, the problem is solved using expansions in power of  $\epsilon$  up to the order  $\epsilon^2$ , in the following form:

$$u = \epsilon U_{-\infty}(\epsilon x, \zeta, T) + \epsilon u_1(\xi, \zeta, T) + o(\epsilon), \quad (39a)$$

$$v = \epsilon V_{-\infty}(\epsilon x, \zeta, T) + \epsilon v_1(\xi, \zeta, T) + o(\epsilon), \quad (39b)$$

$$s = \epsilon S_{-\infty}(\epsilon x, \zeta, T) + \epsilon s_1(\xi, \zeta, T) \\ + \epsilon^2 s_2(\xi, \zeta, T) + o(\epsilon^2), \quad (39c)$$

$$\begin{Bmatrix} \theta \\ \phi \\ y \end{Bmatrix} = \epsilon^2 \begin{Bmatrix} \theta_2 \\ \phi_2 \\ y_2 \end{Bmatrix} + o(\epsilon^2), \quad (39d)$$

where  $\zeta = \epsilon \eta$ ,  $T = \epsilon \tau$ , and where the quantities  $U_{-\infty}$ ,  $V_{-\infty}$ ,  $S_{-\infty}$  have to be expanded around  $x = 0$ . These expansions (39) are valid inside the preheated zone. Outside the flame zone, one has

$$s_{\pm\infty} = \epsilon S_{\pm\infty}(X, \zeta, T), \\ u_{\pm\infty} = \epsilon U_{\pm\infty}(X, \zeta, T), \\ v_{\pm\infty} = \epsilon V_{\pm\infty}(X, \zeta, T), \quad (40)$$

where  $X = \epsilon x$  and

$$y_{\pm\infty} = \theta_{\pm\infty} = r_{\pm\infty} = 0.$$

The quantities involved in (39) and (40) should

<sup>1</sup> To save notation only one transverse coordinate  $\eta = z/d$  is introduced.

be understood as being  $O(1)$  in the limit  $\beta_2 \rightarrow \infty$ . The subscripts  $-\infty$  and  $+\infty$  denote upstream and downstream constant density regions, respectively. According to the definition of the mass flux  $s$ , one has in these regions

$$s_{-\infty} = u_{-\infty} - \alpha_\tau \quad \text{and}$$

$$s_{+\infty} = (1 - \gamma)(u_{+\infty} - \alpha_\tau). \quad (41)$$

Because all the quantities appearing in (39), labeled with the subscripts 1 or 2, are found to go to zero like  $e^\xi$  when  $\xi \rightarrow -\infty$ , the matching between the upstream constant density zone and the preheated zone is automatically satisfied. The solutions in the preheated zone are coupled to the ones of the downstream constant density zone by the jump conditions (11) through the reactive zone, which can be written in the linearized form as

$$[\theta_\xi + L_Y^{-1} y_\xi]_{0-}^{0+} = 0, \quad (42a)$$

$$\theta_\xi|_{0-} = (\beta_2 \theta_f + \theta_f)/2, \quad (42b)$$

$$-L_X^{-1}[\theta_\xi]_{0-}^{0+} = \sqrt{1 + \Delta} \{(\beta_1 - \beta_2/2)\theta_f - \phi_f/2\}, \quad (42c)$$

where the subscript  $f$  denotes the value at the thin reaction zone. The coefficient  $\sqrt{1 + \Delta}$  in (42c) results from using (17).

The left-hand side of these relations can be evaluated by using the outer equations (34), which reduce, to the order  $\epsilon^2$ , to a quasi-planar and quasi-steady form. One obtains

$$\begin{aligned} & -L_X^{-1}[\phi_\xi]_{0-}^{0+} \\ &= \phi_f \sqrt{1 + \Delta} + \nu_L + \int_0^\infty \{S_{+\infty}(\epsilon \xi') \\ &+ L_X \alpha_{\eta\eta}\} e^{-\xi/L_X \sqrt{1 + \Delta}} d\xi' \\ &+ \nu_L - \int_{-\infty}^0 \{s(\xi') \\ &+ L_X^{-1} \alpha_{\eta\eta}\} e^{\xi/L_X \sqrt{1 + \Delta}} d\xi' + o(\epsilon^2), \end{aligned} \quad (43a)$$

$$\theta_\xi|_{0-} = \theta_f + \int_{-\infty}^0 \{s(\xi') + \alpha_{\eta\eta}\} e^{\xi'} d\xi' + o(\epsilon^2), \quad (43b)$$

$$\begin{aligned} L_Y y_\xi|_{0-} &= -L_Y \int_{-\infty}^0 \{s(\xi') \\ &+ L_Y^{-1} \alpha_{\eta\eta}\} e^{\xi/L_Y} d\xi' + o(\epsilon^2). \end{aligned} \quad (43c)$$

As it is clearly explained in Refs. [12] and [13], the expression of the perturbation of the longitudinal mass flux  $s(\xi')$  inside the preheated zone and  $s_{+\infty}$  in the burned gases can be easily computed to the order  $\epsilon^2$  from the mass conservation equation (36), to obtain

$$\begin{aligned} s &= \epsilon S_{-\infty}(X=0) + \epsilon^2 \xi \partial U_{-\infty}/\partial X|_{X=0} \\ &+ \epsilon^2 \{\alpha_{\eta\eta} - \partial U_{-\infty}/\partial X|_{X=0}\} \\ &+ \ln\{1 + e^\xi \gamma/(1 - \gamma)\} + o(\epsilon^2) \end{aligned} \quad (44a)$$

for  $\xi < 0$  and

$$\begin{aligned} s_{+\infty} &= \epsilon S_{+\infty}(X=0) + \epsilon^2 \xi \{\gamma \alpha_{\eta\eta} \\ &+ (1 - \gamma) \partial U_{-\infty}/\partial X|_{X=0}\} \\ &+ o(\epsilon^2) \end{aligned} \quad (44b)$$

for  $\xi > 0$ , with  $S_{+\infty}(X=0) = s(\xi=0)$  and where according to (41)

$$\epsilon S_{+\infty}(X=0) = (1 - \gamma)\{u_{+\infty}(X=0) - \alpha_\tau\}, \quad (45a)$$

$$\epsilon S_{-\infty}(X=0) = u_{-\infty}(X=0) - \alpha_\tau. \quad (45b)$$

The two relations (43b) and (43c) together with Eq. (42a) give the usual values of the modification of the combustion temperature and of the heat flux leaving the reaction zone toward the fresh mixture [12, 16],

$$\begin{aligned} \beta_2 \theta_f &= -l \{\nabla^2 \alpha - \partial u_{-\infty}/\partial x|_{x=0}\} \frac{1 - \gamma}{\gamma} \\ &\times \int_0^{\gamma/(1 - \gamma)} dx \frac{\ln(1 + x)}{x}, \end{aligned} \quad (46)$$

where  $l = O(1)$ , is given by (33),

$$\begin{aligned} \theta_\xi|_{0-} &= \{u_{-\infty}|_{x=0} - \alpha_\tau\} \\ &+ \{\nabla^2 \alpha - \partial u_{-\infty}/\partial x|_{x=0}\} \frac{1}{\gamma} \ln \frac{1}{(1 - \gamma)}, \end{aligned} \quad (47)$$

where  $\nabla^2\alpha$  denotes the transverse Laplacian of  $\alpha$ . By using (44a) and (44b), Eq. (43a) can be written as

$$L_X^{-1}\phi\xi|_{0-}^{0+} = \Phi_f\sqrt{1+\Delta} + (1+\Delta)^{-1/2}\{u_{-\infty}|_{x=0} - \alpha_f\} + \nabla^2\alpha - \partial u_{-\infty}/\partial x|_{x=0}\} K \quad (48)$$

with

$$K \equiv \frac{\nu_L}{L_X\sqrt{1+\Delta}} \left( \frac{\gamma}{L_X\sqrt{1+\Delta}} + \ln \frac{1}{1-\gamma} \right) + \frac{1}{L_X\sqrt{1+\Delta}} + (\nu_L) - \int_{-\infty}^0 \times \ln \left( 1 + \frac{\gamma}{1-\gamma} e^{\xi'} \right) e^{\xi' L_X\sqrt{1+\Delta}} d\xi'. \quad (48')$$

Then, relation (42c) provides the expression of  $\phi_f$ :

$$\frac{3}{2}\Phi_f = (\beta_1 - \beta_2/2)\theta_f - \{u_{-\infty}|_{x=0} - \alpha_f\} - \frac{K}{\sqrt{1+\Delta}} \{ \nabla^2\alpha - \partial u_{-\infty}/\partial x|_{x=0} \}. \quad (49)$$

By using now relation (42b) and the results (46), (47), (49), one obtains the linear equation (50) for the evolution of the front described in the next section.

#### 4. FRONT DYNAMICS

The linear equation for the evolution of the front of a flame sustained by the kinetic scheme A has a form identical to the case of a one-step overall reaction [12], but with a different expression of the Markstein number  $\mathcal{L}$ :

$$\frac{\partial \alpha}{\partial t} = u_{-\infty} + (\mathcal{L}/d) \{ \nabla^2\alpha - \partial u_{-\infty}/\partial x \}, \quad (50)$$

where  $u_{-\infty}$  is the value (at the front) of the normal component of the upstream flow. The Markstein length corresponding to the kinetic scheme A was calculated for the slow recombination regime in

the preceding section, where we obtained

$$\mathcal{L}/d = \left( 1 + \frac{1}{3(1+\Delta)} \right)^{-1} \left\{ \frac{1}{\gamma} \ln \frac{1}{1-\gamma} + (\beta_2 + \beta_1) \frac{(L_Y - 1)(1-\gamma)}{3\gamma} \cdot \int_0^{\gamma/(1-\gamma)} \frac{\ln(1+x)}{x} dx + \frac{K}{\sqrt{1+\Delta}} \right\}, \quad (51)$$

to be compared with the expression

$$\mathcal{L}/d = \frac{1}{\gamma} \ln \frac{1}{1-\gamma} + \beta \frac{L_Y - 1}{2} \frac{(1-\gamma)}{\gamma} \int_0^{\gamma/(1-\gamma)} \frac{\ln(1+x)}{x} dx \quad (52)$$

for the one-step overall reaction [12] with a reduced overall activation energy (Zeldovich number)  $\beta$ .

As already mentioned in the Introduction, the linear equation (50) for the front evolution has been generalized to cases where the amplitude of the front corrugations are finite, if they have small "curvature" [13]. The result can be written as the modification of the normal burning velocity in the form

$$u_n - u_L = -\mathcal{L} \left( \frac{1}{\sigma} \frac{d\sigma}{dt} \right), \quad (53)$$

where  $\mathcal{L}$  has the same value as in the linear case;  $\sigma$  is the element of the front surface, whose relative rate of change times  $\mathcal{L}$  equals the difference between the laminar flame speed  $u_L$  in the planar case and the actual normal burning velocity  $u_n$ . The effects of chemical kinetics and transport properties of the reactive mixture appear in (53) through  $\mathcal{L}$ . The effects of the geometrical configuration of the front and of the flow are measured by the total stretch  $(1/\sigma)(d\sigma/dt)$ . This total stretch results from the curvature of the front  $u_L/\bar{R}$  ( $\bar{R}$  is the local mean radius of curvature of the front) and from the inhomogeneity of the upstream gas flow

“measured” by the rate of strain tensor  $\nabla u_{-\infty}$  at the front [13]. Thus one obtains

$$u_n - u_L = \mathcal{L}(u_L/\bar{R} + \mathbf{n} \cdot \nabla u_{-\infty} \cdot \mathbf{n}), \quad (54)$$

where  $\mathbf{n}$  is the unit vector normal to the flame front. The relations (53) and (54) are general, as long as the weak stretch assumption holds, and they can be used for any flow configuration, for example, for spherical converging flames, planar fronts in stagnation point flow, and turbulent flames. Equations (53) and (54) are still valid for the flame model studied in this paper, provided that the expression (51) is used.

The result (51) that has been obtained in the slow recombination regime will be discussed in the following section, but we will present here its form in two interesting limiting cases:

- i. When the recombination rate increases leading to the merged regime,  $\Delta_0 \rightarrow \infty$  and  $\Delta \rightarrow \infty$ . In this limit  $K = \ln[1/(1 - \gamma)]$  [see Eq. (48b)] and thus (51) takes the form

$$\begin{aligned} \lim_{\Delta_0 \rightarrow \infty} (\mathcal{L}/d) = & \frac{1}{\gamma} \ln \frac{1}{1 - \gamma} \\ & + (\beta_1 + \beta_2) \frac{(L_Y - 1)(1 - \gamma)}{3\gamma} \\ & \times \int_0^{\gamma/(1-\gamma)} \frac{\ln(1+x)}{x} dx. \end{aligned} \quad (55)$$

Notice that in this limit, the diffusive properties of the chain carrier do not affect the dynamical properties of the flame. When compared to the one-step case (52), the overall activation energy  $(2/3)(E_1 + E_2)$  appearing in Eq. (55) has the same value as for the laminar flame speed in the same regime.

- ii. When the recombination rate decreases to zero,  $\Delta_0 \rightarrow 0$  and  $\Delta \rightarrow 0$ , and

$$\begin{aligned} K \rightarrow & \frac{1}{L_X} + L_X \int_{-\infty}^0 e^{\xi' L_X} \\ & \times \ln \left( 1 + \frac{\gamma}{1 - \gamma} e^{\xi'} \right) d\xi', \end{aligned}$$

and the corresponding expression of  $(\mathcal{L}/d)$  is

obtained from (51). Let us write this expression in the case where the Lewis number  $L_X$  of the chain carrier is close to unity. In this case  $|L_X - 1|$  can be considered as a small number compared to unity and we can expand the expression of  $(\mathcal{L}/d)$  linearly in  $L_X - 1$  to obtain, after some simple algebra,

$$|L_X - 1| < 1,$$

$$\begin{aligned} \lim_{\Delta_0 \rightarrow 0} (\mathcal{L}/d) = & \frac{1}{\gamma} \ln \frac{1}{1 - \gamma} + \frac{1}{4} \{(\beta_2 + \beta_1) \\ & \times (L_Y - 1) + (L_X - 1)\} \frac{1 - \gamma}{\gamma} \\ & \times \int_0^{\gamma/(1-\gamma)} \frac{\ln(1+x)}{x} dx. \end{aligned} \quad (56)$$

The result (50) and (51) can be used as in Ref. [16] to investigate the cellular threshold of planar fronts propagating downward. It is not necessary to reproduce here the analysis because it follows exactly the original one [16] (developed for one-step overall reactions). The corresponding results for the present kinetic model can be obtained directly from those of Ref. [16] provided the expression (51) for  $\mathcal{L}$  is used instead of (52). Let us simply recall that flame stability is enhanced by increasing  $\mathcal{L}/d$ .

The analysis presented in Section 3, leading to the results (50) and (52), was devoted to tridimensional and unsteady effects involving space and time scales larger than the transmit time  $\tau_t$  and the thickness  $d$  of the flame ( $\tau_t \sim 10^{-4}$  s and  $d \sim 10^{-2}$  cm at ordinary conditions).

The tridimensional and unsteady effects involving scales  $\tau_t$  and  $d$  can be also studied without many difficulties only if we restrict the analysis to the diffusive thermal model, where the effects of the gas expansion are neglected ( $\gamma = 0$ ) [7]. This model, which neglects the convective transport phenomena in the tangential directions, is not realistic for gaseous combustion but can nevertheless be useful for investigating the mechanism of instabilities that can possibly be produced by the diffusion processes. In particular, this model is appropriated to study planar disturbances of planar fronts in gases.



From the previous studies [2, 7] developed for a one-step overall reaction model, it is known that a Hopf bifurcation is predicted to appear for Lewis number well above the unity,  $L_Y > 1$ . This instability, associated with the time scale  $\tau_i$ , has been used to interpret the spinning waves observed in solid combustion [1, 2] as well as the pulsating fronts observed at flameholders [1, 2]. In order to investigate the effects of the diffusion of the intermediate species upon this instability mechanism, we have carried out the stability analysis of a flame sustained by the kinetic scheme A in the diffusive thermal approximation. The analysis follows closely the method presented in Ref. [7], and will not be reproduced here, where only the final result is given. If  $\sigma$  and  $k$  are, respectively, the growth rate and the wave number of the perturbations, with a  $\tau$  and  $\eta$  dependence of the form  $\exp(\sigma\tau + ik\eta)$ , the following expression of the dispersion relation is obtained:

$$\begin{aligned} & \beta_2(L_Y - 1)(E_1/E_2 \\ & + \Gamma_X/L_X\sqrt{1 + \Delta})\Gamma^{-2}(\Gamma - 1 - 2\omega) \\ & = (L_X - \Gamma_X/\sqrt{1 + \Delta}) + (59\Gamma) \\ & \times (1 + 2\Gamma_X/L_X\sqrt{1 + \Delta}); \end{aligned} \quad (57)$$

here

$$\begin{aligned} \Gamma &= \sqrt{1 + 4(\omega + k^2)} \\ \text{and} \quad \Gamma_X &= \sqrt{L_X^2(1 + \Delta) + 4(\omega L_X + k^2)}. \end{aligned} \quad (58)$$

The result (57) must be compared to the following result obtained for the one-step overall reaction:

$$\frac{\beta(L_Y - 1)}{2} (\Gamma - 1 - 2\omega)/\Gamma^2 = (1 - \Gamma). \quad (59)$$

According to Eqs. (51) and (57), the dynamical properties of the flame front is controlled by four parameters. The diffusion coefficients of the limiting component and of the radical appear through  $\beta_2(L_Y - 1)$  and  $L_X$ , respectively. The recombina-

tion reaction rate appears through  $\Delta$ , which contains also the Lewis number of the radical and the flame speed [see Eq. (14)]. Finally the activation energy of the initiating reaction appears through  $E_1/E_2$ . The dispersion relation (57) reduces to the one-step case (59) in the limit of a fast recombination ( $\Delta \rightarrow \infty$ ) with an effective reduced activation energy

$$\beta = \frac{2}{3} \beta_2 \left( \frac{E_1}{E_2} + 1 \right).$$

This is consistent with Eq. (55), which corresponds in fact to the large wavelengths limit when the gas expansion is neglected ( $\gamma = 0$ ). In the limit of a negligible recombination reaction ( $\Delta = 0$ ), the dispersion relation (58) cannot be reduced to the one-step overall reaction case (59), but for large wavelengths one recovers the result of Eq. (56) with  $\gamma = 0$ .

Thus, the general dispersion relation (57) is much more complex than for the one overall step model. Hopf and steady bifurcations can be easily predicted and the corresponding limits of stability can be obtained from Eq. (57) for each particular flame.

## 5. DISCUSSION OF THE RESULTS

The purpose of this study was to analyze the effects of multiple kinetics and of the diffusive properties of the radicals on the dynamical properties of the flame. We have limited our analysis to a simplified kinetic scheme involving a fast non-branching chain reaction that converts the main reactant into products, coupled with two slower reactions: a chain initiation and a chain breaking, recombination, reaction. As we have indicated in the Introduction, the methods of analysis presented in this study can be used to describe specific flames, as, for example, the halogen-hydrogen flames.

We began by a description of the changes in the steady planar flame structure with increasing values of the recombination rate constant. In all cases the flame propagation velocity is determined by the fast chain reaction. This one takes place in a thin reaction zone at a rate proportional to the

radical concentration. This concentration is determined by the balance between radical production, recombination, and convective and diffusive transport effects. The radical production is due to the initiation reaction and it is localized in the same thin reaction zone where the chain reaction takes place. The radical can be transported out of the production zone by diffusion and will be consumed there by the recombination reaction.

At moderately high flame temperature  $T_d > T_b > T_b^*$ , or equivalently at small values of recombination constant, we recover the results obtained previously by Librovich and Istratov [23], in which the flame propagation velocity turns out to be independent of the diffusive properties of the radical.

The relative importance of the recombination reaction changes with flame temperature, and as a consequence there are also important changes of the flame propagation velocity with the flame temperature. If we define an overall activation energy for the flame propagation velocity as

$$E_{\text{eff}}/RT_b = d(\ln s_L)/d(\ln T_b)$$

and if the thermal effects of dissociation are neglected, we find that this overall activation energy takes the value  $(E_1 + E_2)/2$  for moderately large flame temperatures, when the recombination reaction can be neglected. Due to the effect of the recombination reaction, the effective activation energy increases when the temperature decreases. Through the slow recombination regime, the overall activation energy increases first to a value equal to  $(E_1/2 + 3E_2/4)$  for  $n = 2$ , and  $2(E_1 + E_2)/3$  for  $n = 1$ , and then increases again through the merged regime, to a final value equal to  $(E_2 + E_1/2)$  for  $n = 2$ , and  $E_1 + E_2$  for  $n = 1$ . These last values correspond to low values of the flame temperature  $T_b < T^{**}$  when the steady state approximation can be used for the radical.

On the other limit, for very high flame temperature  $T_b > T_d$ , the endothermic effects of the radical production can no more be ignored as soon as the mass fraction of the radical becomes of the order of  $1/\beta_1$ . As can be inferred from the analysis of Appendix III, the effective activation energy decreases there below the value  $(E_1 + E_2)/2$ .

Notice that  $\Omega_3^*$  [see Eq. (9)] and  $\Omega_3^{**}$  [see Eq. (I.8)], which determine the cross-over temperatures  $T_b^*$  and  $T_b^{**}$ , are strongly dependent on the flame temperature.

The flame temperature can be changed, for example, by dilution of the reactant mixture with an inert species. Figure 3 shows the domains of the different regimes.

We have also shown in the paper how the dynamical properties of the flame can be analyzed in the cases when the radical recombination reaction is not fast enough to prevent the radical from diffusing to the preheated zone. In this case we have found the effect on the flame dynamics of the diffusive properties of the radical, represented by an arbitrary value of its Lewis number. In order to obtain an analytical expression for the dispersion relation, giving the growth rate of the perturbations for arbitrary values of their wavelengths, we used the thermal diffusive model for the flame for  $n = 1$ . However, we also obtained the expression for the Markstein length in the realistic case when the effects of the gas expansion are fully taken into account.

On the high flame temperatures side of the slow recombination region, when the effects of the radical recombination can be neglected, the dynamical flame properties are depending on the radical diffusion and cannot reduce to those of a flame supported by a one-step Arrhenius reaction. Nevertheless, for Lewis number of the radical close to unity, the Markstein number reduces to the one of a one-step reaction with an effective activation energy equal to  $(E_1 + E_2)/2$  [see Eq. (56)]. On the opposite, low flame temperatures, side of the slow recombination regime, when we enter the merged flame regime, the dependence of flame dynamics on the diffusive properties of the radical disappears, and the effective activation energy equals  $2(E_1 + E_2)/3$  [see Eq. (55)].

The dynamical properties of the flame remain independent of the diffusive properties of the radical for lower flame temperatures, in the merged regime, when the radical recombination reaction is fast enough, compared with the production reaction, when the radicals are not able to diffuse out of the thin production zone. In this merged flame regime, the flame properties can be

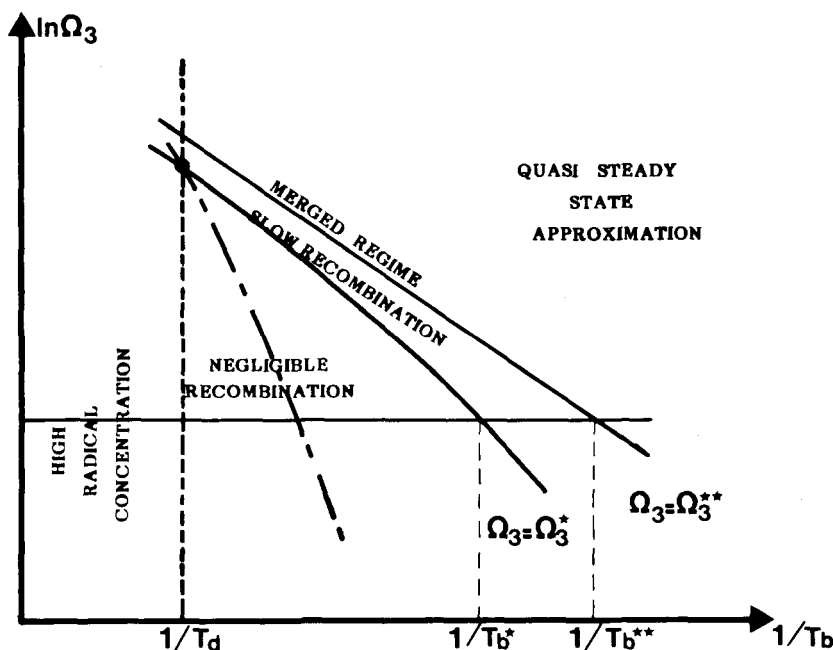


Fig. 3. Domain of the different regimes in the plane  $\ln \Omega_3 - 1/T_b$ . Notice that when, as in the ordinary cases,  $\Omega_3$  varies like pressure, this phase plane corresponds to a pressure-temperature plane.

described by modeling the reaction by means of an effective overall one-step reaction with a large activation energy that depends on the flame temperature  $2(E_1 + E_2)/3 < E_{\text{eff}} < (E_1 + E_2)$ . For sufficiently low values of the flame temperature the rate of radical recombination reaction is large compared with the radical production rate. Then the radical follows the steady state approximation, and we recover the classical results for the flame dynamics associated with a one-step Arrhenius reaction of fixed activation energy,  $E_{\text{eff}} = (E_1 + E_2)$ .

## APPENDIX I

We give here estimates for the radical concentration,  $X_f$ , at the thin reaction zone, and also for the production terms in the conservation equations.

Let  $d = \rho D_T / s_L$  be the characteristic size of the flame thickness: Then (see Fig. 1)  $d/\beta_2$  is the thickness of the reaction zone, because the chain reaction is quenched if  $(T_b - T)$  becomes large compared with  $(T_b - T_u)/\beta_2$ , and  $Y_u/\beta_2$  measures

the variation of the mass fraction of the main reactant in the reaction zone. The convective terms can now be shown to be of the order of  $1/\beta_2$  relative to the diffusive terms, and thus negligible in the thin chain reaction zone.

In the regime analyzed in detail in this paper, the rate of radical recombination,  $\rho Z_3 Y_u^{n-1}$ , is slow enough that radical recombination takes place in zones of thickness  $d$ , outside its production zone in the thin chain reaction zone; the relative changes in  $X$  in this production zone are of the order of  $1/\beta_2$ .

A first relation between the estimates of  $d$  and  $X_f$  is provided by balancing the terms representing diffusion and reactant consumption in (1a):

$$\rho D_Y (Y_u/\beta_2)(\beta_2/d)^2 \sim \rho_b \Omega_2 X_f \beta_2^{-2}. \quad (\text{I.1})$$

The term representing the consumption of the main reactant due to the radical producing reaction,  $\rho_b \Omega_1 Y_u/\beta_2$ , is negligible compared with the terms in (I.1).

A second relation, to estimate  $d$  and  $X_f$ , is

provided by the balance of diffusion and the radical production in the equation for  $X$ :

$$\rho D_X (X_f/\beta_2)(\beta_2/d)^2 \sim \rho_b \Omega_1 (Y_u/\beta_2) \quad (I.2)$$

valid as long as the radical recombination term  $\rho Z_3 X_f^n$  is negligible, or at most of the order of the production term.

From (I.1) and (I.2), we obtain the estimate

$$c_f = X_f/Y_u \sim (\beta_2^{\nu-1} \Omega_1/\Omega_2)^{1/2} \sim (\delta \beta_2^{\nu-1})^{1/2} \quad (I.3)$$

for the peak of the radical concentration. We can use (I.3) to justify the neglect of the radical production term in the conservation equation for the main reactant, when  $\delta = \Omega_1/\Omega_2$  is small compared with unity.

We can neglect the recombination term in the thin radical production zone as long as it is smaller than or of the order of  $1/\beta_2$  times the radical production term. In the main part of this paper we are concerned with the notable limiting case in which the ratio of the two reaction terms is of the order of  $1/\beta_2$ : namely, for values of  $\Omega_3$ , defined by  $\Omega_3 = (Z_{-1} + Z'_3) Y_u^{n-1}$ , such that

$$\Omega_3 Y_u (X_f/Y_u)^n / (\Omega_1 Y_u / \beta_2) \sim 1/\beta_2, \quad (I.4)$$

or equivalently, for values of  $\Omega_3 = O(\Omega_3^*)$ , where

$$\Omega_3^* = \beta_2^{-2+(1-\nu)n/2} \Omega_1^{1-n/2} \Omega_2^{n/2}. \quad (I.5)$$

When  $\Omega_3 = O(\Omega_3^*)$ , the radical recombination term can be neglected in the main thin reaction zone, but not in the outer convective-diffusive zones, when solving the conservation equation for  $X$ .

When  $\Omega_3$  is increased above  $\Omega_3^*$  to make the radical recombination of the same order as the radical production in the thin reaction zone,  $X$  becomes negligible outside the thin zone, and its variation inside is of the order of  $X$  itself. This corresponds to the merged flame regime, for which we can still neglect the radical production and recombination reactions in (1a) and (1c), but both must be retained in thin reaction zone, when solving (1b). The merged flame regime corresponds to values of  $\Omega_3$  such that

$$\begin{aligned} \rho D_X X_f (\beta_2/d)^2 &\sim \rho_b \Omega_1 (Y_u/\beta_2) \\ &\sim \rho_b \Omega_3 Y_u (X_f/Y_u)^n, \end{aligned} \quad (I.6)$$

which together with (I.1) gives

$$c_f = X_f/Y_u \sim (\beta_2^{\nu-2} \Omega_1/\Omega_2)^{1/2} \sim (\delta \beta_2^{\nu-2})^{1/2} \quad (I.7)$$

and the corresponding characteristic value  $\Omega_3^{**}$ ,

$$\Omega_3^{**} = \beta_2^{-1+(2-\nu)n/2} \Omega_1^{1-n/2} \Omega_2^{n/2}, \quad (I.8)$$

of  $\Omega_3$  in the merged flame regime.

For values of  $\Omega_3 \gg \Omega_3^{**}$  we can use the steady state assumption for the radical to calculate  $X$ , or equivalently we can also neglect the radical diffusion term in the thin reaction zone.

Notice also that (I.1) and (I.2) provide the following estimate for the flame burning rate  $s_L = \rho D_T/d$ ,

$$s_L \sim (\rho D_T)^{1/2} \beta_2^{-(\nu+3)/4} \rho_b^{1/2} (\Omega_1 \Omega_2)^{1/4}, \quad (I.9)$$

in the slow recombination regime. Similarly (I.1) and (I.7) lead to the estimate

$$s_L \sim (\rho D_T)^{1/2} \beta_2^{-1-\nu/4} \rho_b^{1/2} (\Omega_1 \Omega_2)^{1/4} \quad (I.10)$$

for the flame burning rate in the merged flame regimes.

These estimates determine the flame speed aside from a factor of order unity, which depends on the Lewis numbers and on the ratio  $\Omega_3/\Omega_3^*$ , in the recombination regime, or on the ratio  $\Omega_3/\Omega_3^{**}$ , in the merged flame regime. This factor will be determined in the main text for  $\Omega_3/\Omega_3^* \sim 1$ , while in Appendix II we show how to calculate the corresponding factor for the merged regime, when  $\Omega_3/\Omega_3^{**} \sim 1$ .

Notice that the ratios of the frequency factors  $\Omega_1, \Omega_2$  are very sensitively dependent on the flame temperature  $T_b$ , while  $\Omega_3$  is roughly independent of  $T_b$ , although growing faster with the pressure than  $\Omega_1$  and  $\Omega_2$ . For this reason, when we decrease the flame temperature, by diluting the reactant with an inert species, we go from the slow recombination regime to the merged regime, and finally, for large values of  $\Omega_3/\Omega_3^{**}$ , to the quasi-steady state approximation for the radical  $X$ .

The effects of radical production in the energy equation need only be taken into account for large values of  $T_b$  such that

$$\rho_b \Omega_1 (Y_u/\beta_2) \sim \beta_2^{-1} \rho_b \Omega_2 X_f \beta_2^{-\nu} \quad (I.11)$$

when due to the endothermicity of the radical

dissociation reaction we find a slowing down of the flame velocity. The analysis of this regime is presented in Appendix III.

## APPENDIX II: THE MERGED FLAME REGIME

We have indicated in Appendix I that for values of the flame temperature  $T_b$ , close to a "cross-over" value  $T_b^{**}$ , such that  $\Omega_3 = \Omega_3^{**}$ , the recombination reaction is fast enough to be confined, like the radical and the other reactions, to a thin zone, of the order of  $d/\beta_2$ , on the hot side of the flame. The radical concentration is so small that the effects of the radical producing and recombining reactions can be neglected in the equations of conservation of energy and mass of the main reactant.

Downstream of the thin reaction zone, we have equilibrium, associated with the approximations indicated above. Namely, for  $x > 0$

$$y_L = c_L = \theta_L - 1 = 0. \quad (\text{II.1})$$

Upstream of the thin zone, for  $x < 0$ , we have chemically frozen flow, so that

$$c_L = 0 \quad y_L = 1 - \exp(xL_Y/d), \quad \theta_L = \exp(x/d). \quad (\text{II.2})$$

In the thin reaction zone, located around  $x = 0$ , where  $x\beta_2/d = \xi = O(1)$ , the convective terms are of the order of  $1/\beta_2$ , relative to the remaining terms, and can thus be neglected for large values of  $\beta_2$ . In addition, the Arrhenius exponent can be linearised around  $T_b$ , because  $(T_b - T_L)/T_b$  is small,  $O(RT_b/E_2)$ , in the reaction zone.

Then the equations that describe, in first approximation for  $\beta_2 \gg 1$ , the temperature, and concentration profiles in the reaction zone take the form

$$\rho D_y \frac{d^2 y_L}{dx^2} = -\rho D_T \frac{d^2 \theta_L}{dx^2} = \rho_b \Omega_2 c_L y_L e^{\beta_2(\theta-1)}, \quad (\text{II.3})$$

$$\rho D_X \frac{d^2 c_L}{dx^2} = -\rho_b \Omega_1 y e^{\beta_1(\theta-1)} + \rho_b \Omega_3 c_L^n, \quad (\text{II.4})$$

to be solved with the boundary conditions

$$\beta x/d \rightarrow \infty: \quad y_L = c_L = \theta_L - 1 = 0 \quad (\text{II.5})$$

and

$$\begin{aligned} \beta x/d \rightarrow -\infty: \quad c_L &= y_L + xL_Y/d \\ &= \theta_L - 1 - x/d = 0 \end{aligned} \quad (\text{II.6})$$

that result from the matching conditions with the outer solutions (II.1) and (II.2).

Notice that (II.3), (5), and (6) lead to the relation  $y_L = (1 - \theta_L)L_Y$ , valid in the reaction zone.

The inner problem (B.3) and (6) can be rewritten in a universal form,

$$u_{\xi\xi} = \tilde{\Lambda} \chi u^\nu e^{-u}, \quad (\text{II.7})$$

$$\chi_{\xi\xi} = \tilde{\Lambda} (-u e^{-uE_1/E_2} + K \chi^n), \quad (\text{II.8})$$

$$\xi \rightarrow \infty: \quad u = \chi = 0, \quad (\text{II.9a})$$

$$\xi \rightarrow -\infty: \quad u + \xi = \chi = 0 \quad (\text{II.9b})$$

in terms of the variables

$$u = \beta_2(1 - \theta_L), \quad \chi = c_L/c_{Lc}, \quad \xi = x\beta_2/d, \quad (\text{II.10})$$

where

$$c_{Lc} = L_Y^{(1-\nu)/2} L_X^{1/2} \beta_2^{-1+\nu/2} (\Omega_1/\Omega_2)^{1/2} \quad (\text{II.11})$$

turns out to be, as (I.3) indicates, the characteristic value of  $c_L$ , in this regime.

Two additional parameters appear in Eqs. (II.7)–(II.9):

$$\tilde{K} = L_X^{n/2} L_Y^{-1+(1-\nu)n/2} \Omega_3/\Omega_3^{**} \quad (\text{II.12})$$

of order unity in the merged regime; and  $\tilde{\Lambda}$ , the flame speed eigenvalue,

$$\tilde{\Lambda} = K^{1/n} (1 + nE_1/E_2)^{1+\nu+1/n/2} \Gamma_{\nu+1/n}. \quad (\text{II.13})$$

The solution of the problem (II.7)–(II.9), needing numerical integration, provides  $\tilde{\Lambda}$ , and hence the flame burning rate per unit flame surface  $s_L$ , as a function of  $\tilde{K}$ , or, equivalently, of the flame temperature  $T_b$  and pressure.

It is important to indicate that the same relation,  $\tilde{\Lambda}(\tilde{K})$ , can be used when unsteady and wrinkling effects modify the outer transport zone, as long as they are not strong enough to affect the thin reaction zone. The only change required is to replace  $T_b$  in Eqs. (II.12) and (13) by the real

flame temperature  $T_f$  just downstream of the thin reaction zone;  $T_f \neq T_b$ , as a consequence of the unsteady and wrinkling effects.

We do not include in this paper the results of the numerical integration of (II.7)–(II.9), but we simply give the asymptotic form of the relation  $\tilde{\Lambda}(\tilde{K})$  for large and small values of  $\tilde{K}$ .

Namely, for large  $\tilde{K}$ , one obtains

$$\tilde{\Lambda} = L_Y^{(1+\nu)/2} L_X^{1/2} \beta_2^{-2-\nu/2} \times (\Omega_1 \Omega_2)^{1/2} \rho_b \rho D_T / s_L^2, \quad (\text{II.14})$$

corresponding to Eq. (8) in the main text. It results from the quasi-steady state approximation for the radical

$$\tilde{K} \chi^n = u \exp(-u E_1 / E_2). \quad (\text{II.15})$$

For  $\tilde{K} \ll 1$  the flame structure is identical to that of the slow recombination regime. That is, we have a radical production zone, where the radical recombination term can be neglected and  $\chi$  approximated by a constant, and outer recombination zones, of thickness, in  $\xi$ , of the order of  $\tilde{K}^{-1/2} \gg 1$ . The analysis leads to the relation

$$\tilde{\Lambda} = \{8\tilde{K}/b^2(n+1)\}^{1/(2+n)} / (2\Gamma_\nu)^{(n+1)/(n+2)}, \quad (\text{II.16})$$

where  $b = b(E_1/E_2)$  is defined after Eq. (11d) of the main text, and  $\Gamma_\nu$  is the gamma function of argument  $\nu$ .

### APPENDIX III: INCIPIENT THERMAL EFFECTS OF RADICAL PRODUCTION

For values of  $\Omega_1/\Omega_2 = \delta = O(1/\beta_2^{1+\nu})$ , the thermal effects of the radical production, reaction can no longer be neglected. These moderately large values of  $\delta$  are obtained for large flame temperatures, and then the effects of the recombination reaction are negligible.

When  $\delta = O(1/\beta_2^{1+\nu})$  the radical concentration is large enough to lead to changes in the flame temperature of the order of  $RT_b^2/E_2$ . These produce changes by factors of order unity, in the flame burning rate  $s_L$  and in the radical concentration  $c_{fL}$ , from the values  $s_{L0}$  and  $c_{fL0}$ , given by

(19a) and (19b), calculated without the thermal effects of the radical dissociation.

The analysis of this regime, of incipient thermal effects of dissociation, can be carried out in a way similar to that used for describing the effects of heat losses in flame propagation [19]. The first significant effect is a lowering of the flame temperature  $T_b$ ; this can be calculated by combining Eqs. (1a)–(1c) to eliminate the chemical production terms, and then integrating the resulting equation from  $-\infty$  to  $\infty$ . Thus we obtain

$$T_f = T_u + Q_2 Y_u / c_p - (Q_2 - Q_1) X_f' / c_p, \quad (\text{III.1})$$

or equivalently,

$$T_f = T_b - (Q_2 - Q_1) X_f' / c_p. \quad (\text{III.2})$$

Here  $T_f$  and  $X_f'$  are the new flame temperature and flame value of the radical concentration.

Notice that  $(Q_2 - Q_1)$  is positive, because the first reaction is endothermic. Then, the new flame temperature is lower than  $T_b$ , due to the thermal effect of the radical production.

The structure of the thin reaction zone is not modified by the small dissociation effects and, therefore, the jump relations (11b) and (11d) are still valid if

- i. We replace  $T_b$  and the value of  $X_f$  appearing there by the new values  $T_f$  and  $X_f'$  to be calculated below.
- ii. To calculate the new gradients of temperature and concentration just upstream of the thin reaction zone (they are zero downstream) we must introduce the factors  $\sigma = s_L/s_{L0}$  and  $\sigma\kappa = s_L X_f' / s_{L0} X_f$  to account for the effect of the change in flame velocity.

The jump conditions (11b) and (11d) then lead to the relations

$$\sigma = \kappa^{1/2} e^{-u/2}, \quad (\text{III.3b})$$

$$\sigma\kappa = \kappa^{-1/2} e^{u/2} e^{-uE_1/E_2}, \quad (\text{III.3c})$$

where  $u = E_2(T_b - T_f)/RT_b^2$  is given according to (III.2) by

$$u = \lambda\kappa \quad (\text{III.4})$$

and the parameter  $\lambda$ , which characterizes this

regime of incipient thermal effects of the radical dissociation, is defined by

$$\lambda = \beta_2 X_f / Y_u = \beta_2 (\delta C / B)^{1/2}. \quad (\text{III.5})$$

Equations (III.3) and (III.4) determine the new flame speed,  $\sigma$ , and radical concentration  $\kappa$ , as well as the new flame temperature,  $u$ , as a function of  $\lambda$ . For example,  $u$  is given by the equation

$$u \exp\{(E_1/E_2 - 1)u/2\} = \lambda, \quad (\text{III.6})$$

and then

$$s_L/s_{L0} = \sigma = \exp\{-(E_1/E_2 + 1)u/4\}, \quad (\text{III.7})$$

$$X_f'/X_f = \kappa = \exp\{-(E_1/E_2 - 1)u/2\}. \quad (\text{III.8})$$

These relations show how  $\sigma$  decreases with increasing values of  $\lambda$ . Thus the effective activation energy, for the deflagration speed, changes again slightly in this regime.

*This work was supported by the E.E.C. Contract no. EN3E0084-F and by the French-Spanish agreement for Scientific Cooperation through the "Actions Intégrées 83-559 and 84-088. We also acknowledge partial support of the work of the first author by the Spanish CAICYT under project no. 2291-83.*

## REFERENCES

- Sivashinsky, G. I., *Ann. Rev. Fluid. Mech.* 15:179-199 (1983).
- Clavin, P., *Prog. in Energy and Combust. Sci.* 11:1-59 (1985).
- Clavin, P., *Prog. in Astronautics and Aeronautics* 95:1-33 (1984).
- Zeldovich, Ya. B., and Frank-Kamenetskii, D. A., *Acta Phys. Chim. URSS*. IX.2:341-350 (1938).
- Bush, W. B., and Fendell, F. E., *Combust. Sci. Tech.* 2:421-428 (1970).
- Sivashinsky, G. I., *Acta Astronautica* 4:1177-1206 (1977).
- Joulin, G., and Clavin, P., *Combust. Flame* 40:139-153 (1979).
- Barenblatt, G. I., Zeldovich, Ya. B., and Istratov, A. G., *Zf. Prikl. Mekh. Tekh. Fiz.* 2:21-26 (1962).
- Darrieus, G., unpublished, 1938.
- Landau, L., *Acta Physicochim, URSS*. 19:77-85 (1944).
- Markstein, G. H., *Nonsteady Flame Propagation*, AGARD Monograph 75, Pergamon Press, New York, 1964.
- Clavin, P., and Williams, F. A., *J. Fluid. Mech.* 116:251-282 (1982).
- Clavin, P., and Joulin, G., *J. Phys. Lett.* 44:L1-12 (1983).
- Matalon, M., and Matkowsky, B. J., *J. Fluid Mech.* 124:239-259 (1982).
- Karlowitz, B., Denniston, J. R., Knapschafer, D. H., and Wells, F. E., *Fourth (International) Symposium on Combustion*, The Williams and Wilkins Co., Baltimore, 1953, pp. 613-620.
- Pelcé, P., and Clavin, P., *J. Fluid Mech.* 124:219-237 (1982).
- Garcia, P., Nicoli, C., and Clavin, P., *Combust. Sci. and Tech.* 42:87-109 (1984).
- Clavin, P., and Nicoli, C., *Combust. Flame* 60:1-14 (1985).
- Joulin, G., and Clavin, P., *Acta Astronautica* 3:223-240 (1976).
- Adams, G., and Stocks, G. V., *Fourth (International) Symposium on Combustion*, The Williams and Wilkins Co., Baltimore, 1953, pp. 239-240.
- Spalding, D. B., *Phil. Trans. R. Soc. London A* 249:1-25 (1956).
- Zeldovich, Ya. B., *Kinetika i Kataliz* 2:305-318 (1961).
- Istratov, A. G., and Librovich, V. B., *Zh. Prikl. Mat. Tekhn. Fiz.* 1:68-75 (1962).
- Bodenstein, M. Z., *Physick. Chem.* 85:329 (1913).
- Hirschfelder, J. O., Curtiss, C. F., and Cambell, D. E., University of Wisconsin, Rep. No CM-756, 1952.
- Von Kármán, T., and Penner, S. S., *Selected Combustion Problems*, Butterworths, London, 1954, pp. 5-41.
- Benson, S. W., *J. Chem. Phys.* 20:1605 (1952).
- Millan, G., and Da Riva, I., *Eighth Symposium (International) on Combustion*, The Williams and Wilkins Co., Baltimore, 1962, pp. 398-411.
- Garcia, P., and Clavin, P., *J. Méc. Théor. Appl.* 2:245-263 (1983).
- Joulin, G., Liñán, A., Lainé, C., Peters, N., and Ludford, G. S. S., to appear in *SIAM J. of Appl. Math.* (1985).
- Liñán, A., and Rodríguez, M., in *Combustion and Non-Linear Phenomena* (P. Clavin, B. Larrourou, and P. Pelcé, Eds.), Les Editions de Physique, Paris, 1985.
- Clavin, P., and Liñán, A., *Nonequilibrium Cooperative Phenomena in Physics and Related Fields* M. G. Velard, (Ed.), Plenum Press, New York, 1984, pp. 291-338.
- Liñán, A., T. R. No. 1 for AFOSR Contract No. EOOAR 68-0031, INTA, Madrid, 1971.